Available online at www.sciencedirect.com
ScienceDirect
Earth and Planetary Science Letters 256 (2007) 147–161
EPSL
www.elsevier.com/locate/epsl

Quantifying transient erosion of orogens with detrital thermochronology from syntectonic basin deposits

Jeffrey M. Rahl *, Todd A. Ehlers, Ben A. van der Pluijm

Department of Geological Sciences, University of Michigan, Ann Arbor, MI, 48109-1063, USA

Received 7 July 2006; received in revised form 12 January 2007; accepted 16 January 2007
Available online 24 January 2007
Editor: R.W. Carlson

Abstract

The evolution of an orogen is marked by phases of topographic growth, equilibrium, and decay. During these phases erosion rates vary in response to temporal and spatial changes in climate, topographic relief and slope, and deformation. Detrital thermochronometer cooling-age data collected from syntectonic basin deposits are a promising tool for quantifying erosion histories during orogenic evolution. Previous studies typically assume steady-state erosion for interpreting detrital data, although in many situations this assumption is not justified. Here we present a new numerical modeling approach that predicts thermochronometer cooling ages in a stratigraphic section where sediment is sourced from a region with a temporally variable erosion history. Multiple thermochronometer cooling ages are predicted at different stratigraphic horizons as a function of variable erosion histories, rock cooling rates in the hinterland, and thermophysical material properties and boundary conditions. The modeling approach provides the context for the interpretation of natural data, including geologically realistic situations with a temporally varying erosion rate. The results of three end-member hinterland erosion histories are explored: (1) steady-state erosion; (2) increasing erosion rate with time; and (3) decreasing erosion rate with time. Results indicate that for steady erosion rates between 0.2 and 1.0 mm/yr, up to 30 m.y. will pass following a change in erosion rate before the detrital ages have adjusted to reflect a new erosion regime. In simulations with transient erosion, the estimation of erosion rates from a detrital record using assumption of thermal steady-state will generally be in error, often by as much as −25 to 100%. These results highlight that assumptions of steady erosion in mountain belts should be used with caution. Application of the model to thermochronometer cooling ages preserved in syntectonic sediments sourced from the Nanga Parbat region, Himalaya, illustrates how the transient catchment averaged erosion history can be quantified with detrital thermochronology. In this example, we found that erosion rates increased over the past 20 Ma, from about 1.0 mm/yr to modern rates in the range of 1.5 to 2.0 mm/yr.

Keywords: detrital thermochronology; orogenic erosion; Himalaya; thermal modeling

1. Introduction

Quantifying the long-term erosion of orogenic belts is essential to assess the influence of tectonics and climate on erosion during different stages of an orogen's history. Thermochronologic data (e.g. (U–Th)/He, fission track, $^{40}Ar/^{30}Ar$ data) reflect the thermal history

* Corresponding author. Now at Department of Geology, Washington and Lee University, Lexington, Virginia 24450, USA.
E-mail address: rahlj@wlu.edu (J.M. Rahl).

0012-821X/$ - see front matter © 2007 Elsevier B.V. All rights reserved.
doi:10.1016/j.epsl.2007.01.020

of a rock and therefore provide a valuable tool with which to estimate rates of cooling, often due to erosion. Several different approaches have proved successful for quantifying thermal histories in orogenic belts. For example, inversion of apatite fission-track length distributions [1–4] and age–elevation transects [5–8] both constrain the timing of rock cooling through certain temperatures. Yet, as successful as these approaches have been, their application is limited by a requirement of presently exposed bedrock for study. These techniques are not applicable to ancient settings where only synorogenic sediments are preserved, nor may they be used to constrain the earliest part of orogenesis for which the bedrock material has been eroded (Fig. 1A).

As an alternative, an increasing number of studies have attempted to utilize the thermochronologic record preserved in detrital material [see [9], and references within]. In addition to applications in sedimentary provenance [10–15] and landscape evolution [16–21], detrital thermochronology shows great promise for illuminating the long-term evolution of orogenic belts. Provided that heating from burial within a basin is insufficient to reset a particular thermochronometer, the preserved ages reflect cooling in the source terrane and therefore may be used to constrain the long-term rates of exhumation and erosion [17,22–29].

With detrital approaches increasingly used to quantify rates of erosion and exhumation, it is critical to understand how a given erosional signal will be recorded in the thermochronologic ages of eroded detritus. Although simple interpretations based on steady-state assumptions of the erosion history and thermal field are possible, several factors complicate the problem: (1) the effective closure temperature for

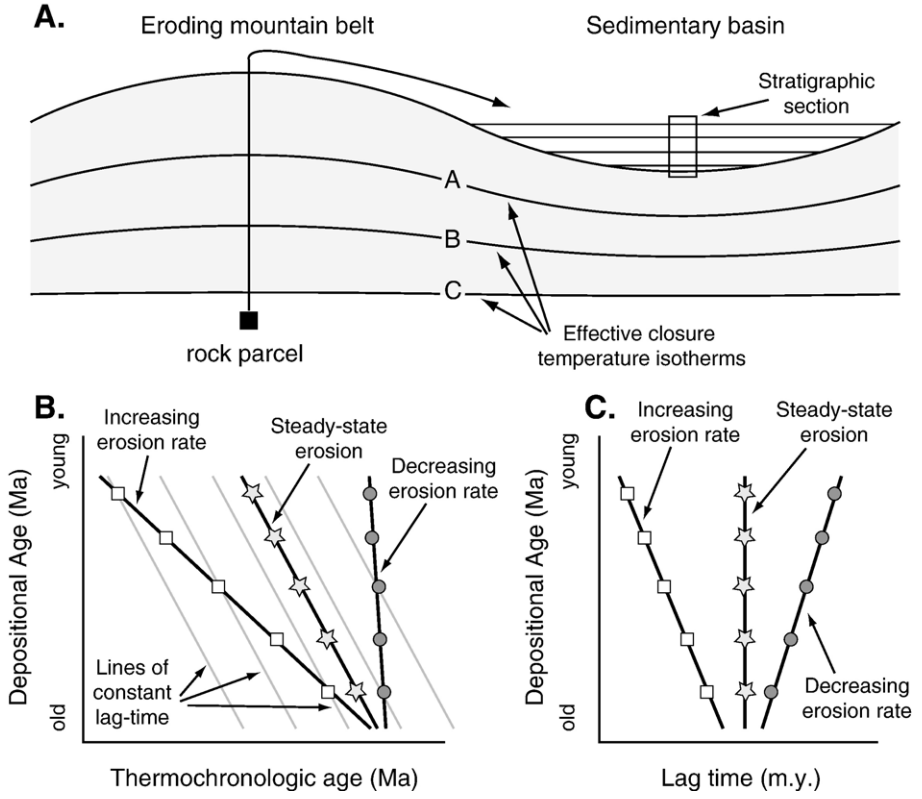

Fig. 1. (A) Schematic upper crustal cross-section of an orogen, showing the position of isotherm. Erosion removes material from the surface and advects material towards the surface. As a given parcel of moves towards the surface, it cools and passes through the effective closure temperature isotherms for the various low-temperature thermochronometer systems (shown schematically here as A, B, and C). This sample may then be deposited in an adjacent sedimentary basin. (B) Ages from a stratigraphic section showing the expected distribution of thermochronometer ages for three separate scenarios. When erosion rates are steady with time (grey stars), each sample will take the same amount of time to reach the surface from its effective closure depth. Ages will young up-section but always "lag" behind the stratigraphic age by a constant amount. In contrast, for an increasing erosion rate (white squares) ages will young faster than the stratigraphic age; for a decreasing erosion rate (dark grey circles), ages will young more slowly than the depositional age. (C) Lag-time (defined as the cooling age minus the stratigraphic age) versus depositional age for the three scenarios.

thermochronometers is not fixed but varies as a function of the cooling rate [30,31]; (2) exhumation rates common in active orogens (>~0.2 mm/yr) result in the upward advection of heat toward the Earth's surface and alter the thermal profile of the crust [32,33]; (3) varying erosion results in a transient thermal field through which samples cool; and (4) the response time of a particular thermochronometer to changes in erosion rate is unique for each system [34]. Because of these complications, numerical models of the thermal effects of erosion represent a powerful tool with which to interpret detrital thermochronologic data and evaluate assumptions of steady-state erosion and subsurface temperatures.

In this contribution, we present a 1D finite element model to investigate how variable erosion rates affect the thermal field of an orogen and the time–temperature histories experienced by the eroded material. Our work provides a framework to interpret thermochronologic data, with a particular emphasis on the analysis of detrital data from syntectonic foreland deposits. Specifically, we present three end-member numerical experiments designed to represent characteristic geologic scenarios: (1) steady-state erosion and exhumation; (2) a rapid step change in erosion rate that might reflect a climatic shift or tectonic event; (3) a gradually changing erosion rate that might correspond to a protracted period of mountain building or steadily decaying topography in an ancient orogen. The scenarios are applicable to interpreting erosion histories from basins located proximal to a single structure such as in a fold and thrust belt, or more distal settings where sediment derived from a wider region is deposited to produce an integrated record of the erosion history. For each model, we investigate how the thermochronologic ages from the eroded material evolve with time and consider how detrital ages can be inverted to reconstruct the erosional history of the source terrane. Finally, we illustrate the value of our approach through application to a published zircon fission-track and white mica $^{40}Ar/^{39}Ar$ data set from the Siwalik Group sediments, Pakistan, that record erosion of the Himalaya [35].

2. Background: erosion, exhumation, and thermochronology

Erosion in tectonically active orogenic belts typically operates at rates ranging from 0.5 to 5 mm/yr [e.g., [36]], advecting both heat and mass towards the surface of the Earth. As individual parcels of rock cool during exhumation, they pass through the "effective closure temperature" isotherms for the various thermochronometric systems and "lock in" ages (Fig. 1A). A number of thermochronometers are available, each sensitive to a unique effective closure temperature. Most relevant to exhumation studies are the low-temperature systems, including (U–Th)/He of apatite and zircon [37,38], fission-track of apatite and zircon [39,40], and Ar/Ar in white mica [29,41]. These systems are sensitive to temperatures ranging from ~60 °C for apatite (U–Th)/He to 350 to 425 °C for white mica [34], conditions typical of the upper 2 to 15 km of the crust.

Thermochronometer ages generally represent the amount of time that has passed since a sample cooled through the effective closure temperature for a particular system. An age may reflect cooling following volcanism or adjacent plutonism, during normal faulting, or due to erosional exhumation. Here, we focus on settings in which exhumation is accomplished solely through erosion. In such cases, thermochronometer ages may be used to estimate the rate of erosion. A simple approach is to assume a geothermal gradient and an effective closure temperature and take the erosion rate as equal to the cooling age divided by the depth of eroded crust. For example, for a typical crustal thermal gradient of 25 °C/km and a zircon fission-track closure temperature of ~250 °C, a zircon fission-track age of 12 Ma would indicate an average erosion rate of about 0.83 mm/yr (10 km of erosion over 12 m.y.). However, numerous thermal modeling studies indicate that assuming an effective closure temperature depth may cause significant errors [33,42–44]. As noted above, rapid erosion alters the thermal structure of the crust by advecting heat toward the surface. For example, Ehlers [32] shows that sustained erosion at a rate of 1 mm/yr may increase temperatures at 10 km depth by nearly 200 °C within 15 m.y. Thus, the depth to the effective closure temperature isotherm, which must be known to estimate the erosion rate, will itself vary with the erosion rate. A second complication is that in detail the effective closure temperature for thermochronometers is not fixed but varies as a function of the cooling rate [30,31]. For example, Reiners and Brandon [34] demonstrate that the effective closure temperature for many thermochronometers may vary by 50 to >100 °C over a range of geologically reasonable cooling rates. Numerical models provide one means to account for these difficulties. For example, Brandon et al. [45] use a 1D thermal model to derive a relationship between thermochronometer age and erosion rate for a thermally re-equilibrated crust [see also [25]].

An important goal is to extend this approach to the stratigraphic record to constrain the long-term erosional history of an orogen. After a rock has been exposed at

the surface, it may be eroded and transported to an adjacent sedimentary basin or more distal repository (Fig. 1A). In detrital thermochronology, a useful quantity is the "lag time" [22], defined as the difference between the depositional and thermochronologic ages. In general, the more rapid the erosion rate, the smaller the lag time. Provided the time between the exposure of a given sample at the surface and deposition is geologically short, the lag time may be used to estimate the erosion rate of its source area at the time of deposition, in the manner described above for bedrock samples. Studies of sedimentary transport suggest that the time from erosion to deposition is typically short, less than 1 m.y. [46–49]. Thus, although in some cases sediment may be temporarily stored within a landscape and then later remobilized [e.g., [13,50]], equating the time of exposure with the time of deposition is reasonable.

For settings with a long and continuous record of deposition, the lag-time approach may be used to document how the erosion rate within the orogen evolved with time [24–27,35,51,52]. The higher the erosion rate, the less time needed to exhume a sample from a given depth, so lag-time is inversely related to the exhumation rate [25]. Jamieson and Beaumont [53] provide a conceptual framework for orogenic belts often invoked to interpret lag-time data [e.g., [26,27,51]]. In this view, orogenic zones are expected to evolve through three states: (1) an early, constructional phase, characterized by an increase in topography and erosion rates; (2) a steady-state phase, with constant relief and erosion rates; and (3) a late destructive or decay phase, characterized by decreasing topography and erosion rates. Each of these scenarios will produce a distinct pattern of ages (Fig. 1B) and lag-times (Fig. 1C) moving up a stratigraphic section [54]. Thus, lag-time variations provide a potential tool with which to identify the long-term erosional history of an orogen.

The estimation of a temporally varying erosion rate is particularly challenging due to transients in the subsurface thermal field. In addition to the problems in estimating the depth to an effective closure temperature isotherm discussed above, a further difficulty arises because the thermal profile of the crust does not respond instantaneously to a change in erosion rate due to the low thermal diffusivity of rock. For example, analytical models indicate that the thermal profile of the crust may take at least 40 m.y. to re-equilibrate in response to an instantaneous 1 mm/yr increase in the rate of erosion or sedimentation [32,33]. Age–elevation transects have documented significant changes (by a factor of 2 to 10) in erosion rates in several mountain belts [e.g., [7,44,55]], so it is likely that few orogens are in a thermal steady-state. Reiners and Brandon [34] show that in response to an instantaneous change to a new steady erosion rate, lower temperature isotherms will approach their new equilibrium value more quickly than higher temperature isotherms. They show that for a step increase in erosion rate from 0 to 1 mm/yr and a fixed temperature basal boundary condition, the effective closure temperature isotherms for the commonly used thermochronometer systems will not approach their new equilibrium depth for 4 to 8 m.y. The equilibration time increases significantly if a basal flux boundary condition is considered [e.g., [32]]. Thus, if the erosion rate changes on shorter timescales (whether continuously or in a series of jumps) the effective closure temperature of the various isotherms will continually be in motion. This effect is due to the transience of the thermal field and is generally not accounted for when transforming thermochronometer ages into erosion rates. For example, the method described above [25,45] calculates an effective closure depth as a function of erosion rate but assumes that a steady thermal field has been achieved.

3. Modeling approach

We use a one-dimensional finite element model [modified from [56 57 58]] to investigate the effect of a variable catchment average erosion rate on the thermal structure of the crust and the thermochronologic signal preserved in the eroded material. The model solves the transient 1D advection–diffusion equation for variable sedimentation and erosion histories using a Galerkin finite-element formulation with implicit time stepping. The model is formulated in a Lagrangian (material) reference frame and tracks material properties and cooling histories during the exhumation process. Thermal–tectonic processes accounted for in this model include: (1) transient and/or steady-state erosion, (2) crustal heating due to radiogenic heat production, (3) variable basal heat flow into the base of the crust, and (4) variable thermophysical properties, including conductivity, density, and heat capacity [see [57], for details of the model]. The thermal model was validated against analytic solutions for the transient 1D advection–diffusion equation for constant erosion rates [59]. Temperature differences between the model and analytic solutions are $\ll 1\%$ for the range of erosion rates considered in this study.

Time–temperature histories of material eroded from the thermal model are stored and used to calculate predicted thermochronometer ages deposited in an adjacent sedimentary basin at different times, assuming

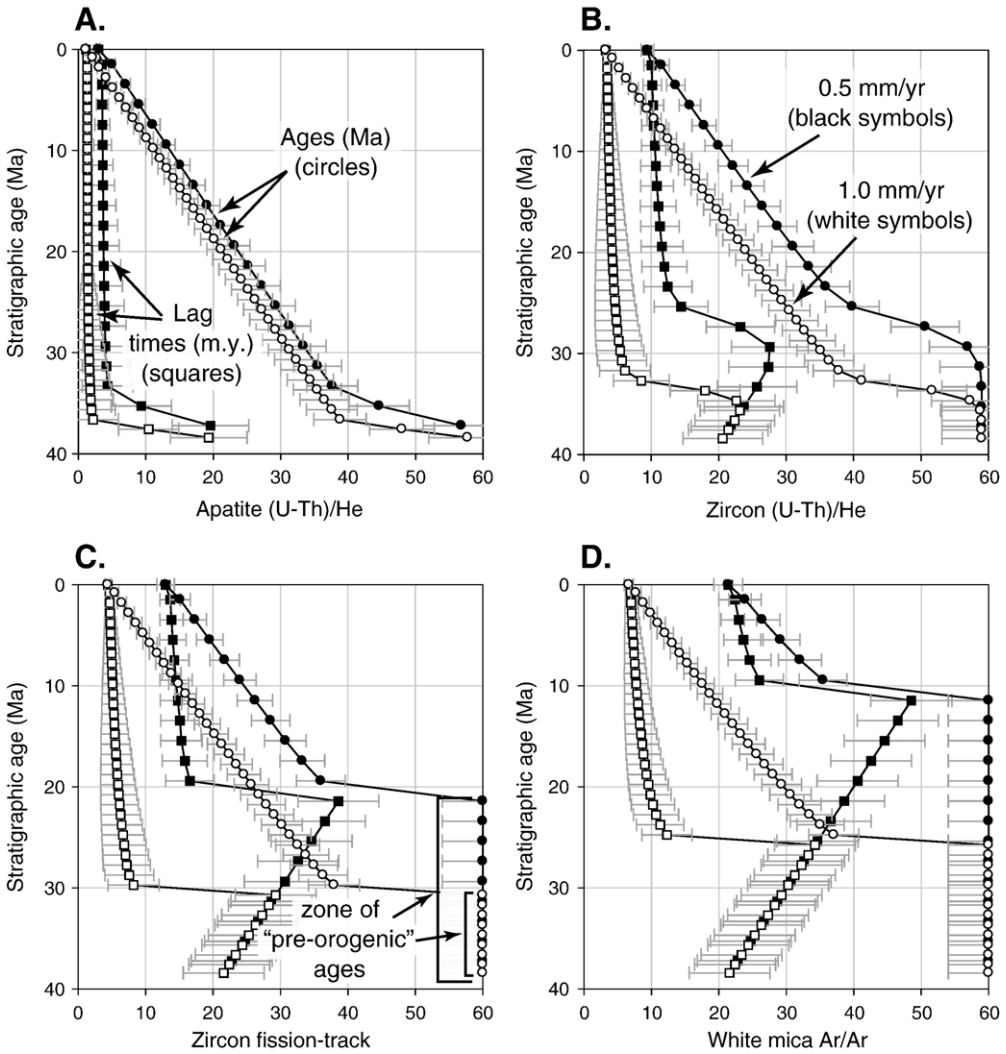

Fig. 2. Thermochronometer ages and lag-times plotted versus stratigraphic age for two steady-state models, at 0.5 mm/yr (black symbols) and 1.0 mm/yr (white symbols). Ages were calculated using a 1D thermal model to predict thermochronometer ages as a function of variable erosion rates. Thermochronometer ages are show with circles, and lag-times indicated by squares. (A) Apatite (U–Th)/He. (B) Zircon (U–Th)/He. (C) Zircon fission-track. (D) White mica Ar/Ar. Errors are assumed to be 10% of the predicted age.

the transport time of sediment to the basin is short. We focus on four thermochronometers well-suited for detrital studies: apatite and zircon (U–Th)/He, zircon fission-track, and white mica Ar/Ar. Ages are calculated using the TERRA thermochronometer age prediction program [60], which uses various established algorithms for cooling rate dependent age prediction. Apatite and zircon (U–Th)/He ages are calculated by solving the transient spherical ingrowth diffusion equation [37] using a spherical finite element model [43,61]. Because a complete model of track annealing in zircon is yet to be developed, TERRA calculates zircon fission-track ages using an effective closure temperature approach [22,31,45,48]. For Ar/Ar ages, we employ a fixed closure temperature of 350 °C. Although in detail the closure temperature will vary with cooling rate, the general results presented and interpreted here are not significantly influenced by our assumed closure temperature.[1]

For each of the simulations discussed here, a thermally equilibrated crustal column with no erosion is held for 20 m.y. prior to the onset of a 40 m.y.

[1] The thermal and age prediction models used in this study are freely available to others upon request. Interested persons should contact the corresponding author (J. Rahl) or T. Ehlers (tehlers@umich.edu).

simulation with erosion. The initial 20 m.y. period allows for rocks in the uppermost crust that originate at temperatures below that of the various effective closure temperatures to have ages that pre-date the beginning of the model simulation. This represents natural settings in which the upper crust must have an age structure prior to the onset of orogenesis and rapid erosion, and allows us to identify exhumed material that originated at temperatures above that of the effective closure temperature for each system. The material that is eroded at each time interval is assumed to be instantaneously transported to an adjacent sedimentary basin. We assume that the basin is insufficiently thick to partially or completely reset the various thermochronometers. Although this assumption may not be valid in very thick sedimentary basins or for thermochronometers with a low closure temperature, such as the apatite (U–Th)/He system, it does reflect common natural conditions. Note also that the modeled results assume that all ages reflect cooling in a single source area. In practice, a sedimentary deposit will contain a mixture of grains derived from multiple areas, each with unique erosional histories. Peak-fitting (e.g., [62]) provides a tool to recognize distinct grain-age components in natural samples.

4. Results

4.1. Steady-state erosion, predicted thermochronometer ages, and lag-times

First, we present the thermochronometer ages and lag-times for several models with steady-state erosion. Fig. 2 shows predicted ages (circles) and lag-times (squares) for sediment derived from models, with steady erosion rates of 0.5 (black) and 1.0 (white) mm/yr plotted against the stratigraphic age. Results are shown for four thermochronometer systems (Fig. 2A–D). All the systems show a similar pattern: the oldest horizons contain material with unreset (60 Ma) and identical ages. Moving upwards in the stratigraphy, at some point the thermochronometer ages quickly decrease and then progressively young towards the top of the stratigraphic section. The lag-times show a similar pattern: lag-times slowly increase in the oldest part of the section before rapidly younging and approaching a constant value in the highest layers of the stratigraphy. The old cooling ages preserved in the lower part of the section are derived from the uppermost crust in the model, from temperatures cooler than the effective closure temperature for each thermochronometer. This zone contains unreset "pre-orogenic" ages (e.g. Fig. 2C) unrelated to the modern episode of exhumation.

Despite the similarities in the overall structure for each of the thermochronometer systems shown in Fig. 2, the differences between the systems and simulations illustrate several important principles. (1) The lower the effective closure temperature of a thermochronometer system, the less sensitive its ages and lag-times are to a change in erosion rate. For example, consider the apatite (U–Th)/He (closure temperature ~70 °C) and zircon fission-track systems (about 250 °C) (Fig. 2A, C, respectively). The apatite (U–Th)/He ages at erosion rates of 1.0 mm/yr are about 2 m.y. younger than those for with an erosion rate of 0.5 mm/yr (Fig. 2A); in contrast, the zircon fission-track ages for the 1.0 mm/yr model are about 10 m.y. younger than for the 0.5 mm/yr model. (2) The thickness of the zone in the stratigraphic column with "pre-orogenic" cooling ages will depend both upon the steady erosion rate and the effective closure temperature of the system. When rates are fast (white symbols), erosion will more quickly remove the portion of crust with "pre-orogenic" cooling ages (e.g. Fig. 2C). Similarly, the thickness of the initial crustal column with "pre-orogenic" ages will increase with the effective closure temperature of a system. Consequently, for these systems a greater amount of time must pass before erosion will expose material with young ages. For example, the 0.5 mm/yr model shows that it takes between 7 m.y. for apatite (U–Th)/He (Fig. 2A) to 30 m.y. for white mica Ar/Ar (Fig. 2D) to strip off the unreset zone of "pre-orogenic" ages. (3) For all the models, the ages will converge on a steady lag-time value that depends on both the thermochronometric system and the steady erosion rate. This lag time decreases with

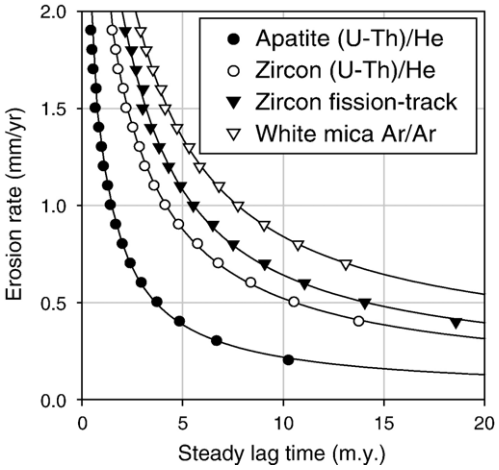

Fig. 3. Steady lag-time versus erosion rate for a steady erosion models for four low-temperature thermochronometers. The data are fit by a third-order inverse polynomial.

effective closure temperature and increases with erosion rate.

The third observation suggests a relationship between the erosion rate and the steady lag-time. To delineate this relationship, a series of simulations were conducted with steady erosion at varying rates (Fig. 3). For each simulation, the steady lag-time is defined as the lag-time for which samples originally 3 km apart in the crustal column have lag-times within 5%. These experiments define the relationship between the model erosion rate and the steady lag-time. Note that as the erosion rate increases the lag-time decreases non-linearly. The relationship shown in Fig. 3 has been applied in a number of studies to interpret orogen erosion histories assuming steady-state erosion. For example, Brandon and others [e.g., [25,27,45]] use the relationship between lag-times and erosion rates to invert a natural thermochronologic dataset to constrain the erosional history of a source terrane. An example of this approach is presented in Fig. 4, which shows zircon fission-track results for three separate experiments: one with steady erosion at a rate of 0.75 mm/yr, one with an increasing erosion rate (from 0 to 1.5 mm/yr over 40 m.y.), and one with decreasing erosion (from 1.5 to 0 mm/yr over 40 m.y.). The simulations predict thermochronometer ages and lag-times (Fig. 4B). Using the relationship between zircon fission-track lag-time and erosion rate defined in Fig. 3, these lag-times can be transformed to get a record of erosion (Fig. 4A). Note that, once the "pre-orogenic" zone is removed, the erosion rate history is successfully reconstructed for the steady-state case. However, this approach produces significant errors when the applied erosion rate varies with time (see below).

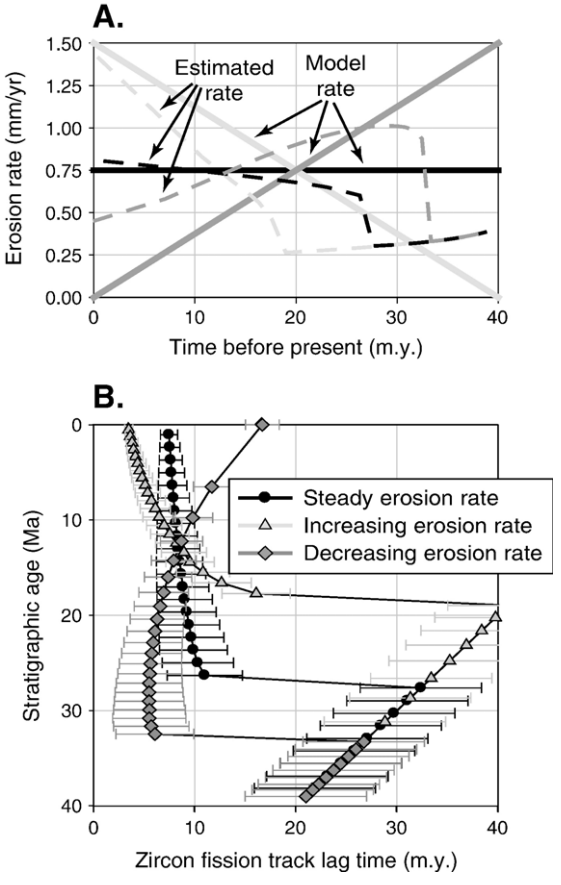

Fig. 4. (A) Actual (solid line) and estimated (dashed line) erosion rate histories for three models, illustrating the differences between a steady-state, increasing, and decreasing erosional history. All three models have equal amounts of total erosion. The estimated rates are determined by inverting the lag-time from the zircon-fission track ages (shown in B), using the erosion-rate to lag-time relationship defined by Fig. 3. Errors are assumed to be 10% of the predicted age. (B) Zircon fission-track lag-times.

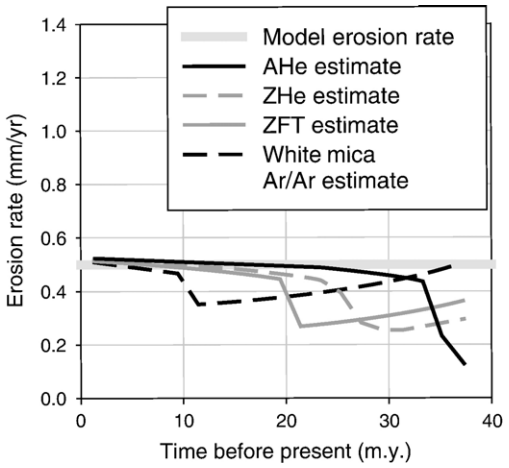

Fig. 5. Estimated (thin lines) and actual (thick grey line) erosion rate for steady state erosion at a rate of 0.5 mm/yr. Estimated rates determined by using the lag times from each of the four thermochronometers. Once "reset" rocks from each system reach the surface, the estimated erosion rates converge on the true rate. AHe=apatite (U–Th)/He, ZHe=zircon (U–Th)/He, ZFT=zircon fission track.

4.2. Errors in estimating erosion rate from lag-time

4.2.1. Steady state case

A useful conceptual end-member model for mountain belts is that of steady-state erosion [53]. Although there are different aspects of an orogen that may remain steady with time [see [63]], we focus here on an exhumational steady-state in which the rate of erosion remains fixed with time. Exhumational steady-state is expected for mature yet active mountain belts, after an orogen has achieved a thermal steady-state; proposed examples include the Central European Alps [27] and Taiwan [63].

Fig. 5 presents results from the steady-state simulation with a constant erosion rate of 0.5 mm/yr shown in Fig. 2. The lag-time for the four thermochronometer systems were inverted to estimate erosion rates using the steady-state lag-time to erosion rate relationship depicted in Fig. 3. Initially, the estimated erosion rates (thin lines) are in error by as much as 50% in the first 10 to 30 m.y. of erosion, but with time the estimates converge towards the true value (thick grey line). The erroneous estimates correspond to lag-times derived from the "pre-orogenic" zone. An accurate estimate of the erosion rate is not possible until the lag-times are obtained from deep samples initially below the closure temperature for a given system. Again, the amount of time it takes to erode through this zone will depend upon the erosion rate and the particular thermochronometer system. For example, at a rate of 0.5 mm/yr, it takes nearly 20 m.y. of erosion before the zircon fission-track ages at the surface will reflect the applied erosion rate. Additional simulations (not shown) confirm that at higher erosion rates, less time is needed to strip away the crustal section containing "pre-orogenic" ages.

4.2.2. Linearly changing rates

The steady-state simulations confirm that, provided sufficient time has passed to allow for removal of the unreset material, the lag-times will approach a steady value that can be inverted to estimate the erosion rate. However, erosion rates generally vary with time due to changes in tectonic and/or climatic forcing. Fig. 6A shows results from simulations with linearly increasing erosion rates; additional plots showing results form linearly changing models are available in the Supplementary Material. Increasing erosion rate simulations correspond to the "constructional" phase of orogenesis [sensu [53]] and may be applicable to settings such as the Himalaya where continued convergence builds topography and gradually increases erosion rates. Decreasing erosion rate simulations might represent decaying orogens such as the Appalachians.

In contrast to the steady-state models discussed above, inversion of lag-times generally does a poorer job of estimating the long-term erosional history of an orogen with a variable erosion rate. Differences between the model input and measured erosion rates range from between 50 to 200% after the unreset zone has been removed (see Supplementary Material Fig. 1). These errors in erosion measured erosion rates result from the thermal field having to continually adjust to a changing erosion rate. In these circumstances it is not possible for the lag-times to perfectly reconstruct erosion rates because the depth to the closure temperature isotherm is continually changing. Nonetheless, these models do highlight important results: (1) the lower the effective closure temperature, the better a thermochronometer will estimate the long-term erosional history. For example, the estimated erosion rate from the apatite (U–Th)/He system (solid black line in Fig. 6A) comes closest to approximating the applied erosion rate (thick grey line). (2) The transformation of lag-time to erosion rate tends to underestimate increasing erosion rates and overestimate decreasing erosion rates. (3) The more rapid the change in erosion rate, the greater the error. (4) For simulations with peak erosion rates at 0.5 mm/yr, the "pre-orogenic" zone is not eroded through for most thermochronometers. For example, Supplementary

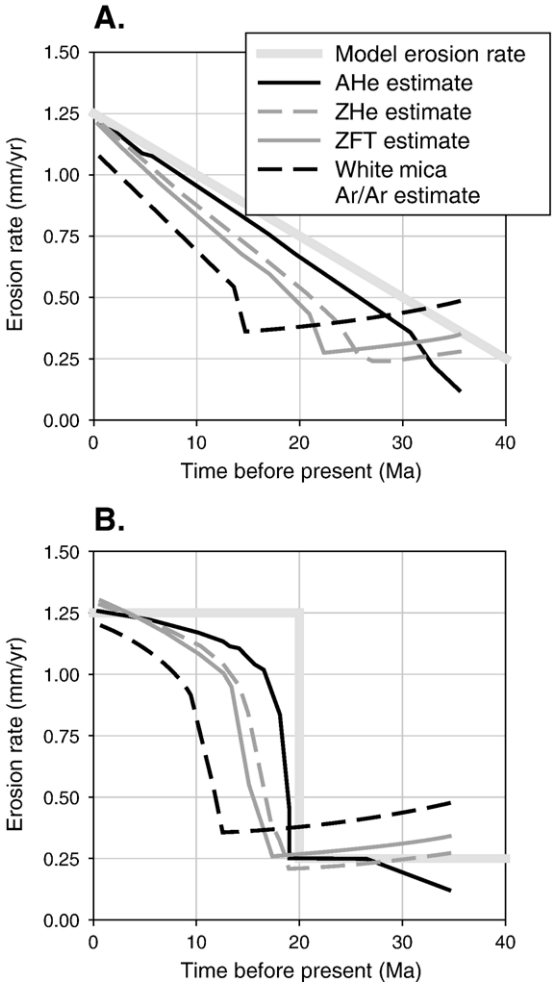

Fig. 6. Estimated and actual erosion rates for transient erosion models, comparing a with a linearly varying change (A) with a step increase (B). Lower closure temperature systems (such as apatite (U–Th)/He) are more sensitive to the different erosional histories, while higher temperature systems like white mica Ar/Ar predict similar histories despite the actual differences in erosion rate between models.

Material Fig. 1B shows that estimates from reset zircon fission-track ages are not obtained until 4 m.y. before the end of the simulation, and young white mica Ar/Ar ages are never exposed. This is important because it may be common in natural settings, where orogenic erosion rates are often less than 0.5 mm/yr [e.g., [36]].

4.2.3. Step-changes in erosion rates

Although erosion rates may vary slowly over million-year time-scales, geologically instantaneous changes may occur as well. For example, motion on a thrust system may generate topography and increase local erosion rates, or sudden climatic shifts may quickly alter precipitation and erosion rates. Fig. 6A and B presents an example of the effect on the time-scale of the change in erosion rate by comparing step-changes with a linearly varying models. Additional examples are presented in the Supplementary Material.

The estimated erosion rates for the step-change models are different from those for the continually varying simulation, particularly for the lowest closure temperature systems. In all the simulations, the apatite (U–Th)/He system (solid black line) once again most accurately approximates the applied erosion rate. As the effective closure temperature increases, each system becomes less sensitive to the changes in erosion rate. For instance, consider the white mica Ar/Ar system (dashed black line) for the step-increase and linear increase (Fig. 6A and B). Despite a widely different erosional history, the reconstructed erosional history for the two experiments is broadly similar. As a general rule, the lower the closure temperature, the more sensitive a system is to changes in erosion rate. For example, in Fig. 6, the erosion rate increases from 0.25 to 1.25 mm/yr. Although the apatite (U–Th)/He estimate reflects this full variation over 30 m.y., the white mica Ar/Ar estimates only range from about from 0.35 to 1.1–1.2 mm/yr. The higher the effective closure temperature, the more "damped" the erosion rate signal.

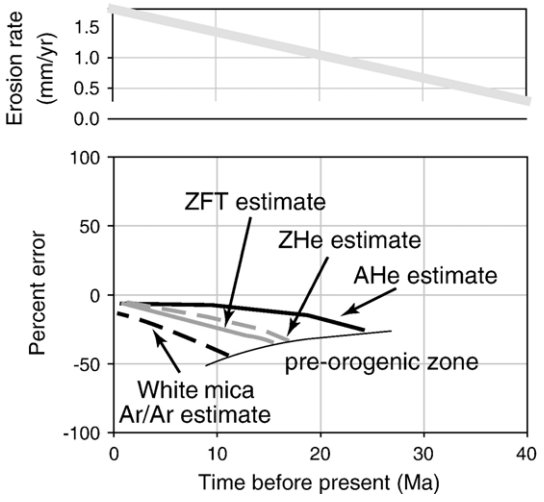

Fig. 7. Erosional histories and percent error in erosion rate estimates for the linearly increasing history described in Fig. 4. In cases with transient erosion histories, transforming lag-times into erosion rates will lead to significant errors.

5. Discussion

5.1. Lag times and erosion rates

Previous studies have inverted observed lag-times from a stratigraphic column to constrain the erosion history of the source terrane, but our numerical experiments indicate that under many circumstances such estimates will be in error. This approach works well when: (1) the unreset material with "pre-orogenic" ages is first removed, and (2) the long-term erosion rate remains steady, for at least 5 to 30 m.y. at rates of 0.5 mm/yr and at least 3 to 20 m.y. at rates of 1.0 mm/yr. However, transient erosion rates are more likely to be the norm. In these cases, using steady-state lag-times to estimate erosion rates may produce large errors. For example, Fig. 7 shows results from the increasing erosion rate experiment described in Fig. 4. For this model, the predicted rates made using the steady lag-time assumption underestimates the actual erosion rate by at least ~25%. The magnitude of error for the case of a deceleration in erosion rates may be as large as 100% (see Supplementary Material Fig. 3). Therefore, although the erosion rate estimates quickly converge on the actual solution within 5 to 20 m.y. in the steady case, the simulations demonstrate that estimated erosion rates will be significant for transient erosion. This result emphasizes the value of numerical modeling in calculating erosion rates from detrital thermochronologic data.

5.2. Precision of erosion rate estimates

As noted by others [e.g., [25,34]] and confirmed here, a non-linear relationship exists between the lag-time and the erosion rate of the source terrane. Lag-times are less responsive to changes in erosion rate at higher rates (Fig. 3). Consequently, there is a limit as to how precisely erosion rates may be constrained in rapidly eroding mountain belts. For example, consider the relationship between the steady-lag time and the erosion rate for the zircon (U–Th)/He system (white circles in Fig. 3). At a modest orogenic erosion rate of

0.5 mm/yr, the model predicts a lag time of about 11 m.y. If the error on a given zircon (U–Th)/He age determination is 10%, this results in a 1 m.y. error on the lag-time for a sample from modern river sediment. This range is consistent with erosion rates between ~0.45 and 0.55 mm/yr, or about a 0.10 mm/yr window. If the erosion rate is doubled to 1.0 mm/yr, the model predicts a steady lag-time for the zircon helium system of about 4 m.y. For a similar 10% error, the model predicts erosion rates between ~0.9 to ~1.2 mm/yr, a range 3 times greater than that for the 0.5 mm/yr erosion rate. Although this problem is less significant for modern and very young samples, the errors on thermochronologic age determinations increase significantly going back in geologic time. For instance, consider the case of a 25 Ma zircon (U–Th)/He age from a 30 Ma stratigraphic horizon. The lag-time of 5 m.y. suggests an erosion rate of about 0.9 mm/yr. However, a 10% error on the age determination extends the range of the lag-time from 2.5 to 7.5 Ma. These values are consistent with erosion rates from 0.65 to 1.5 mm/yr, an error of 70–160%.

The decreased sensitivity of steady lag-times to changes in erosion rates is greatest at high erosion rates and for low temperature thermochronometer systems, because in these situations lag-times change little with large changes in erosion rate (Figs. 2 and 3). Therefore, for rapidly eroding mountain belts, higher closure temperature systems are better suited for quantifying erosion rates. However, these systems also have a significant disadvantage: because their effective closure temperatures reside deep in the crust, it may take a long time before material with reset, young ages reaches the surface. For example, with steady erosion of 1 mm/yr, it will take about 20 m.y. before rocks that reside at the closure depth for the white mica Ar/Ar system are exposed (e.g., Fig. 2D). Because of this lengthy delay, the early record of these ages will not constrain the modern exhumation history of the orogen. In slowly eroding mountain belts, the ages for the high temperature systems may contain no information on rates and only provide an upper limit on the integrated thickness of eroded rock. In such settings, lower temperature thermochronometer systems are better suited to constrain rates of orogenic erosion.

5.3. An example from the Siwalik Group from the Himalaya

The results and discussion above indicate that numerical simulations provide an important tool to constrain erosion histories from detrital thermochronologic data. Ideally, a studied area will have a long, continuous stratigraphic section containing multiple datable phases, such as zircon and white mica; a clear link to a source area; and the material should have a cooling history dominated by erosional exhumation.

To illustrate, we focus on two previously published data sets from the Siwalik Group in the Western Himalaya to investigate whether the Nanga Parbat region has been undergoing steady or transient erosion over the past 20 to 40 m.y. (Fig. 8). The Siwalik Group preserves fluvial sediments deposited by the paleo-Indus River from 18–14 Ma [64]. Detrital zircon fission-track [35] and white mica Ar/Ar [65] data have been obtained from this group, and Cerveny et al. [35] present additional results from modern river deposits that extend the zircon fission-track record to the present. Cerveny et al. [35] note the existence of relatively young zircons (lag time <10 m.y.) in all of their samples, and bedrock zircon fission-track data from throughout the catchment [66] indicate that the only area with young (<10 Ma) zircon fission-track ages is the Nanga Parbat region. Similarly, Najman et al. [65] present petrographic and white mica cooling data that further support the Nanga Parbat region as an important source for at least some of Siwalik Group sediment. Although the region is tectonically active, mapping and structural analysis has failed to identify large-scale extensional structures capable of exhuming the rocks from depth [e.g., [67]]. Consequently, numerous workers have concluded that erosion represents the dominant exhumation process, in addition to controlling the metamorphic, geomorphic, and structural evolution of the region [68–71]. Thus, this setting is ideal for detrital thermochronologic study, with a lengthy record of deposition and a clear source area dominated by erosional exhumation.

We used standard peak-fitting procedures [e.g., [62]] to deconvolve the zircon fission-track grain-age distributions of Cerveny et al. [35] into multiple components. We focus here on the youngest peak component, which represents the most rapidly exhuming source area, and has an age ranging from 28 Ma for the 18 Ma deposits to about 2 Ma in modern sediments (large white circles in Fig. 8B). The dataset provides an excellent example of a decreasing lag-time moving stratigraphically upsection [54], a pattern expected for the "constructive" phase of orogenesis and suggesting an increasing erosion rate with time. Additional information is provided by detrital white mica Ar/Ar data from the same section [65]. Their grain age distributions generally contain 18 to 30 grains, too few to identify statistically significant component peaks. Nonetheless, the range of ages presented in their data provides an important constraint on exhumation processes.

To better interpret these data, we ran a series of simulations (with model parameters in Table 1 in the Supplementary Material) for different erosional histories (Fig. 8A) to compare predicted ages and lag-times with the observations. For the first simulation, we used an erosional history estimated by inverting the zircon fission-track lag-time data itself. A best-fit line calculated for the lag-time data was transformed into an erosional history using the lag-time to erosion–rate relationship defined by Fig. 3 (green line in Fig. 8A). This result indicates a history in which the erosion rate has increased exponentially with time, reaching modern values in excess of 2.0 mm/yr. However, the results from the simulations discussed earlier demonstrate that transforming lag-times into erosion rates will yield erroneous results if the source terrane was not eroding in a steady fashion. In fact, the predicted zircon fission-track and white mica Ar/Ar lag-times for this simulation (green squares in Fig. 8) fail to reproduce the observations by as much as 5 to 10 m.y. As an alternative, we attempted to fit the data with a series of steady-state erosion simulations, one of which is shown in Fig 8 (red triangles). Although these results generally fit the Ar/Ar well, they fail to capture the decreasing lag-time observed in the zircon fission-track ages (Fig. 8C).

The decreasing lag-time moving stratigraphically upsection suggests an increasing erosion rate with time. We attempted to fit the data with a simple model in which the erosion rate has increased linearly for the past 40 m.y., with modern values of 1.7 mm/yr (blue circles). The predicted zircon fission-track lag-times match the observed data well, showing a decreasing lag-time upsection. However, these simulations fail to match the white mica Ar/Ar data, which have significantly younger lag-times than the model predictions. The difference is that in this simulation, the unreset material is not completely removed by 20 Ma, and the old "pre-orogenic" ages have significantly greater lag-times. Thus, a fourth simulation was performed, with a similar history for the past 20 m.y. but with greater erosion rates in the period 20 to 40 Ma to ensure sufficient erosion to completely exhume reset white mica Ar/Ar ages. This two-stage model predicts both zircon fission-track and Ar/Ar ages consistent with the observed detrital thermochronologic data (yellow diamonds). The transient thermal modeling approach

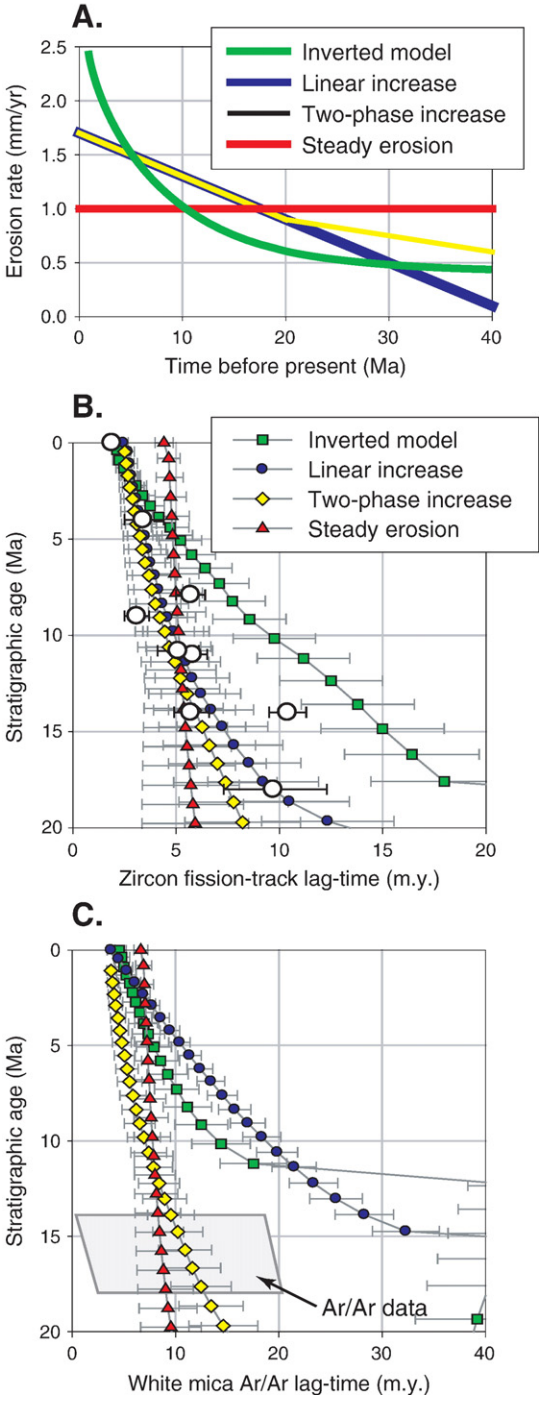

Fig. 8. Detrital thermochronologic data and simulation results for the Siwalik Group sediments in the Pakistan Himalaya. (A) Several modeled erosion histories; lag-times for these simulations are shown in C and D. Four models are investigated: (1) an accelerating erosion rate history determined by inverting the zircon fission-track lag-time data [35] using a steady-state thermal history assumption (green); (2) a steady erosion rate (red); (3) a linear increase from 40 Ma to present (blue); and (4) a two-stage linear increase (yellow). (B) Zircon fission-track lag-times [35] plotted against stratigraphic age (white circles) and predicted lag-times for the erosion histories in B. (C) Predicted white mica Ar/Ar lag-times for the erosion histories in B. Grey background box shows range of observed Ar/Ar ages [65]. Errors on simulation data are assumed to be 10% of the predicted age.

presented here illustrates how detrital thermochronometer data can be used to delineate between different erosion histories. Our interpretation of the Nanga Parbat erosion history from multiple thermochronometer systems would not be possible if a steady-state thermal field was assumed.

Our interpretation that erosion rates increase from about 1.0 mm/yr to modern values of 1.5 to 2.0 mm/yr is consistent with previous workers who suggested an increasing erosion rates in the Nanga Parbat region since 20 Ma [65]. This modern estimate is broadly consistent with petrological estimates for current erosion rates in the range of 2 to 6 mm/yr [72,73]. The results also indicate that the total amount of erosion prior to 18 Ma must have been sufficient to remove the entire zone of unreset white mica Ar ages, because young (lag time <15 Ma) detrital white micas are observed. The model predicts that current white mica Ar/Ar ages should be about 5 Ma, matching the observations of bedrock white mica Ar ages from Nanga Parbat that range from 4 to 6 Ma [74]. Increasing erosion rates have also been inferred in other parts of the orogen, including the central Himalaya [e.g., [75]]. Future studies of detrital thermochronologic data, coupled with numerical models as described here, will help illuminate the long-term erosional history of this and other orogenic belts.

6. Conclusions

The results described here confirm that detrital thermochronology is a powerful tool with which to investigate the long-term, transient, erosional history of orogenic belts. The primary conclusions from this study include:

1) Thermochronometer ages in detrital settings will not reflect a modern erosional episode until the material in the upper crust with existing ages has been removed. The time required to remove this zone of "pre-orogenic" ages depends on the effective closure temperature of the system, the erosion rate, and total duration (and hence magnitude) of erosion.
2) Lag-times vary in response to changes in erosion rate, and therefore may be used to reconstruct the long-term erosional history of an orogen. Although lag-times may be simply inverted to reconstruct erosion rates for steady-state mountain belts, when erosion rates are transient this will lead to errors of up to −25 to 100%. Numerical models represent a valuable tool to construct erosional histories from lag-times and identify non-uniqueness in interpretations from detrital data.
3) Different thermochronometer systems have different sensitivities to changes in erosion rate. Low closure temperature systems, such as apatite (U–Th)/He, respond quickly to abrupt changes in erosion rate. In contrast, higher closure temperature systems, such as white mica Ar/Ar, integrate cooler over a longer period of time and are therefore less sensitive to rapid changes in erosion rate.
4) At rates of 1.0 mm/yr or higher, lag-times become unresponsive to changes in erosion rate. This makes it difficult to accurately estimate fast erosion rates. The problem becomes more significant farther back in time because measurement errors are larger. Low-closure temperature systems are most susceptible to this problem.
5) Numerical simulations of detrital thermochronologic data derived from the Nanga Parbat region indicate increasing erosion rates over the past 20 Ma, from about 1.0 mm/yr to modern rates in the range of 1.5 to 2.0 mm/yr.

Acknowledgements

This work benefited from thoughtful discussion and advice from Phil Armstrong and Dave Whipp. Matthias Bernet performed the peak-fitting for the Cerveny data. Research was supported by a Turner Postdoctoral Fellowship to Rahl at the University of Michigan and NSF grants EAR-0230055 (van der Pluijm), EAR-0409289 and EAR-0544954 (Ehlers), and EAR-0629331 (van der Pluijm, Ehlers, Rahl). This manuscript benefited from a review by Barbara Carrapa.

Appendix A. Supplementary data

Supplementary data associated with this article can be found, in the online version, at doi:10.1016/j.epsl.2007.01.020.

References

[1] P.F. Green, I.R. Duddy, G.M. Laslett, K.A. Hegarty, A.J.W. Gleadow, J.F. Lovering, Thermal annealing of fission tracks in apatite: 4. Quantitative modelling techniques and extension to geological timescales, Chemical Geology. Isotope Geoscience Section 79 (1989) 155–182.
[2] W.D. Carlson, Mechanisms and kinetics of apatite fission-track annealing, American Mineralogist 75 (1990) 1120–1139.
[3] S.D. Willett, Inverse modeling of annealing of fission tracks in apatite: 1. A controlled random search method, American Journal of Science 297 (1997) 939–969.
[4] R. Ketcham, R. Donelick, M. Donelick, AFTSolve: a program for multi-kinetic modeling of apatite fission-track data, American Mineralogist 88 (2003) 929.

[5] P. Fitzgerald, The transantarctic mountains of the southern Victoria land: the application of apatite fission track analysis to a rift shoulder uplift, Tectonics 11 (1992) 634–662.
[6] D. Seward, N.S. Mancktelow, Neogene kinematics of the Central and Western Alps; evidence from fission-track dating, Geology 22 (1994) 803–806.
[7] P.G. Fitzgerald, J.A. Munoz, P.J. Coney, S.L. Baldwin, Asymmetric exhumation across the Pyrenean orogen: implications for the tectonic evolution of a collisional orogen, Earth and Planetary Science Letters 173 (1999) 157–170.
[8] D.F. Stockli, T.A. Dumitru, M.O. McWilliams, K.A. Farley, Cenozoic tectonic evolution of the White Mountains, California and Nevada, Geological Society of America Bulletin 115 (2003) 788–816.
[9] M. Bernet, C. Spiegel, Introduction: detrital thermochronology, in: M. Bernet, C. Spiegel (Eds.), Detrital Thermochronology; Provenance Analysis, Exhumation, and Landscape Evolution of Mountain Belts, Geological Society of America (GSA), Boulder, CO, United States, 2004, pp. 1–6.
[10] A.J. Hurford, A. Carter, The role of fission track dating in discrimination of provenance, in: A.C. Morton, S.P. Todd, P.D. Haughton (Eds.), Developments in Sedimentary Provenance Studies, vol. 57, Geological Society of London Special Publications, London, 1991.
[11] T.R. Ireland, Crustal evolution of New Zealand: evidence from age distributions of detrital zircons in Western Province paragneisses and Torlesse greywacke, Geochimica et Cosmochimica Acta 56 (1992) 911–920.
[12] G.E. Gehrels, W.R. Dickinson, Detrital zircon provenance of Cambrian to Triassic miogeoclinal and eugeoclinal strata in Nevada, American Journal of Science 295 (1995) 18–48.
[13] J.M. Rahl, P.W. Reiners, I.H. Campbell, S. Nicolescu, C.M. Allen, Combined single-grain (U–Th)/He and U/Pb dating of detrital zircons from the Navajo Sandstone, Utah, Geology (Boulder) 31 (2003) 761–764.
[14] I.H. Campbell, P.W. Reiners, C.M. Allen, S. Nicolescu, R. Upadhyay, He–Pb double dating of detrital zircons from the Ganges and Indus Rivers: implication for quantifying sediment recycling and provenance studies, Earth and Planetary Science Letters 237 (2005) 402–432.
[15] G.M. Stock, T.A. Ehlers, K.A. Farley, Where does sediment come from? Quantifying catchment erosion with detrital apatite (U–Th)/He thermochronometry, Geology 34 (2006) 725–728.
[16] P.A. Cawood, A.A. Nemchin, Paleogeographic development of the east Laurentian margin: constraints from U–Pb dating of detrital zircon in the Newfoundland Appalachians, Geological Society of America Bulletin 113 (2001) 1234–1246.
[17] K.W. Ruhl, K.V. Hodges, The use of detrital mineral cooling ages to evaluate steady state assumptions in active orogens: an example from the central Nepalese Himalaya, Tectonics 24 (2005).
[18] I.D. Brewer, D.W. Burbank, K.V. Hodges, Downstream development of a detrital cooling-age signal: insights from $^{40}Ar/^{39}Ar$ muscovite thermochronology in the Nepalese Himalaya, in: S.D. Willett, M.T. Hovius, M.T. Brandon, D.M. Fisher (Eds.), Tectonics, Climate, and Landscape Evolution: GSA Special Paper, vol. 398, Geological Society of America, Boulder, CO, 2005, pp. 321–338.
[19] I.D. Brewer, D.W. Burbank, K.V. Hodges, Modelling detrital cooling-age populations: insights from two Himalayan catchments, Basin Research 15 (2003) 305–320.
[20] C.W. Wobus, K.V. Hodges, K.X. Whipple, Has focused denudation sustained active thrusting at the Himalayan topographic front? Geology 31 (2003) 861–864.
[21] M. Schaller, T.A. Ehlers, Limits to quantifying climate driven changes in denudation rates with cosmogenic radionuclides, Earth and Planetary Science Letters 248 (2006) 153–167.
[22] M.T. Brandon, J.A. Vance, Tectonic evolution of the Cenozoic Olympic subduction complex, Washington State, as deduced from fission track ages for detrital zircons, American Journal of Science 292 (1992) 565–636.
[23] H. von Eynatten, R. Gaupp, J.R. Wijbrans, $^{40}Ar/^{39}Ar$ laserprobe dating of detrital white mica from Cretaceous sediments of the Eastern Alps: evidence for Variscan high-pressure metamorphism and implications for Alpine orogeny, Geology 24 (1996) 691–694.
[24] L. Lonergan, C. Johnson, Reconstructing orogenic exhumation histories using synorogenic zircons and apatites: an example from the Betic Cordillera, SE Spain, Basin Research 10 (1998) 353–364.
[25] J.I. Garver, M.T. Brandon, T.M.K. Roden, P.J.J. Kamp, Exhumation history of orogenic highlands determined by detrital fission-track thermochronology, in: U. Ring, Mark T. Brandon, Gordon S. Lister, Sean D. Willett (Eds.), Exhumation Processes; Normal Faulting, Ductile Flow and Erosion, Geological Society Special Publications, vol. 154, Geological Society of London, London, United Kingdom, 1999, pp. 283–304.
[26] B. Carrapa, J. Wijbrans, G. Bertotti, Episodic exhumation in the Western Alps, Geology 31 (2003) 601–604.
[27] M. Bernet, M. Zattin, J.I. Garver, M.T. Brandon, J.A. Vance, Steady-state exhumation of the European Alps, Geology (Boulder) 29 (2001) 35–38.
[28] K.W. Huntington, K. Hodges, A comparative study of detrital mineral and bedrock age-elevations methods for estimating erosion rates, Journal of Geophysical Research — Earth Surface 111 (2006).
[29] K.V. Hodges, K.W. Ruhl, C.W. Wobus, M.S. Pringle, $^{40}Ar/^{39}Ar$ thermochronology of detrital minerals, Reviews in Mineralogy and Geochemistry 58 (2005) 239–257.
[30] M.H. Dodson, Closure temperature in cooling geochronological and petrological systems, Contributions to Mineralogy and Petrology 40 (1973) 259–274.
[31] M.H. Dodson, Theory of cooling ages, in: E. Jager, J.C. Hunziker (Eds.), Lectures in Isotope Geology, Springer-Verlag, Berlin, Germany, 1979, pp. 194–202.
[32] T.A. Ehlers, Crustal thermal processes and the interpretation of thermochronometer data, Reviews in Mineralogy and Geochemistry 58 (2005) 315–350.
[33] N.S. Mancktelow, B. Grasemann, Time-dependent effects of heat advection and topography on cooling histories during erosion, Tectonophysics 270 (1997) 167–195.
[34] P.W. Reiners, M.T. Brandon, Using thermochronology to understand orogenic erosion, Annual Review of Earth and Planetary Sciences 34 (2006) 419–466.
[35] P.F. Cerveny, N.D. Naeser, P.K. Zeitler, C.W. Naeser, M.N. Johnson, History of uplift and relief of the Himalaya during the past 18 million years: evidence from fission-track ages of detrital zircons from sandstones of the Siwalik Group, in: K. Kleinspehn, C. Paola (Eds.), New Perspectives in Basin Analysis, Springer-Verlag, New York, 1988, pp. 43–61.
[36] U. Ring, M.T. Brandon, S.D. Willett, G.S. Lister, Exhumation processes, in: U. Ring, Mark T. Brandon, Gordon S. Lister, Sean D. Willett (Eds.), Exhumation Processes; Normal Faulting, Ductile Flow and Erosion, Geological Society Special Publications, vol. 154, Geological Society of London, London, United Kingdom, 1999, pp. 1–27.

[37] K.A. Farley, Helium diffusion from apatite; general behavior as illustrated by Durango fluorapatite, Journal of Geophysical Research, B, Solid Earth and Planets 105 (2000) 2903–2914.
[38] P.W. Reiners, K.A. Farley, H.J. Hickes, He diffusion and (U–Th)/He thermochronometry of zircon: initial results from Fish Canyon Tuff and Gold Butte, in: Barry P. Kohn, Paul F. Green (Eds.), Low Temperature Thermochronology: from Tectonics to Landscape Evolution, Elsevier, Amsterdam, Netherlands, 2002.
[39] K. Gallagher, R. Brown, C. Johnson, Fission track analysis and its application to geological problems, Annual Review of Earth and Planetary Sciences 26 (1998) 519–572.
[40] T. Tagami, H. Ito, S. Nishimura, Thermal annealing characteristics of spontaneous fission tracks in zircon, Chemical Geology. Isotope Geoscience Section 80 (1990) 159–169.
[41] I. McDougall, T.M. Harrison, Geochronology and Thermochronology by the $^{40}Ar/^{39}Ar$ Method, Second edition, Oxford University Press, Oxford, 1999, 269 pp.
[42] K. Stuwe, L. White, R. Brown, The influence of eroding topography on steady-state isotherms. Applications to fission track analysis, Earth and Planetary Science Letters 124 (1994) 63–74.
[43] T.A. Ehlers, P.A. Armstrong, D.S. Chapman, Normal fault thermal regimes and the interpretation of low-temperature thermochronometers, Physics of the Earth and Planetary Interiors 126 (2001) 179–194.
[44] T.A. Ehlers, S. Willett, P.A. Armstrong, D.S. Chapman, Exhumation of the central Wasatch Mountains, Utah: 2. Thermokinematic model of exhumation, erosion, and thermochronometer interpretation, Journal of Geophysical Research (2003) 12-11–12-18.
[45] M.T. Brandon, M.K. Roden-Tice, J.I. Garver, Late Cenozoic exhumation of the Cascadia accretionary wedge in the Olympic Mountains, Northwest Washington State, Geological Society of America Bulletin 110 (1998) 985–1009.
[46] M. Bernet, M.T. Brandon, J.I. Garver, B. Molitor, Downstream changes of Alpine zircon fission-track ages in the Rhone and Rhine Rivers, Journal of Sedimentary Research 74 (2004) 82–94.
[47] P. Copeland, T.M. Harrison, Episodic rapid uplift in the Himalaya revealed by $^{40}Ar/^{39}Ar$ analysis of detrital K-feldspar and muscovite, Bengal Fan, Geology (Boulder) 18 (1990) 354–357.
[48] R.J. Stewart, M.T. Brandon, Detrital-zircon fission-track ages for the "Hoh Formation": implications for late Cenozoic evolution of the Cascadia subduction wedge, Geological Society of America Bulletin 116 (2004) 60–75.
[49] M.A. Jones, P.L. Heller, E. Roca, M. Garcés, L. Cabrera, Time lag of syntectonic sedimentation across an alluvial basin: theory and example from the Ebro Basin, Spain, Basin Research 16 (2004) 467–488.
[50] S.C. Sherlock, Two-stage erosion and deposition in a continental margin setting: an $^{40}Ar/^{39}Ar$ laserprobe study of offshore detrital white micas in the Norwegian Sea, Journal of the Geological Society of London 158 (2001) 793–799.
[51] C. Spiegel, W. Siebel, J. Kuhlemann, W. Frisch, Toward a comprehensive provenance analysis: a multi-method approach and its implications for the evolution of the Central Alps, in: M. Bernet, C. Spiegel (Eds.), Detrital Thermochronology — Provenance Analysis, Exhumation, and Landscape Evolution of Mountain Belts, Geological Society of America Special Paper, vol. 378, Geological Society of America, Boulder, Colorado, 2004, pp. 37–50.
[52] H. von Eynatten, F. Schlunegger, R. Gaupp, J.R. Wijbrans, Exhumation of the Central Alps; evidence from $^{40}Ar/^{39}Ar$ laserprobe dating of detrital white micas from the Swiss Molasse Basin, Terra Nova 11 (1999) 284–289.
[53] R.A. Jamieson, C. Beaumont, Deformation and metamorphism in convergent orogens: a model for uplift and exhumation of metamorphic terrains, in: J.S. Daly, R.A. Cliff, B.W.D. Yardley (Eds.), Evolution of Metamorphic Belts, vol. 43, Geological Society of London Special Publications, 1989, pp. 117–129.
[54] M. Bernet, J.I. Garver, Fission-track analysis of detrital zircon, Reviews in Mineralogy and Geochemistry 58 (2005) 205–238.
[55] P.W. Reiners, Z. Zhou, T.A. Ehlers, C. Xu, M.T. Brandon, R.A. Donelick, S. Nicolescu, Post-orogenic evolution of the Dabie Shan, eastern China, from (U–Th)/He and fission-track thermochronology, American Journal of Science 303 (2003) 489–518.
[56] P.A. Armstrong, D.S. Chapman, R.H. Funnell, R.G. Allis, P.J. Kamp, Thermal modelling and hydrocarbon generation in an active margin basin: the Taranaki basin, New Zealand, AAPG Bulletin 80 (1996).
[57] P.A. Armstrong, P.J. Kamp, R.G. Allis, D.S. Chapman, Timing of the heat flow high on the Taranaki Peninsula (New Zealand): Evidence from combined apatite fission track age and vitrinite reflectance data, Basin Reseach 9 (1997).
[58] P.A. Armstrong, D.S. Chapman, Combining tectonic and temperature evolution in Taranaki Basin, New Zealand, in: A. Forster, D. Merriam (Eds.), Geothermics in Basin Analysis, Plenum Press, 1999, pp. 151–176.
[59] H.S. Carslaw, J.C. Jaeger, Conduction of Heat in Solids, Second edition, Oxford University Press, Oxford, 1959, 510 pp.
[60] T.A. Ehlers, T. Chaudhri, S. Kumar, C.W. Fuller, S.D. Willett, R.A. Ketcham, M.T. Brandon, D.X. Belton, B.P. Kohn, A.J.W. Gleadow, T.J. Dunai, F.Q. Fu, Computational tools for low-temperature thermochronometer interpretation, Reviews in Mineralogy and Geochemistry 58 (2005) 589–622.
[61] T. Ehlers, K. Farley, Apatite (U–Th)/He thermochronometry: methods and applications to problems in tectonic and surface processes, Earth and Planetary Science Letters 206 (2003) 1–14.
[62] M.T. Brandon, Decomposition of fission-track grain-age distributions, American Journal of Science 292 (1992) 535–564.
[63] S.D. Willett, M.T. Brandon, On steady states in mountain belts, Geology (Boulder) 30 (2002) 175–178.
[64] N.M. Johnson, J. Stix, L. Tauxe, P.F. Cerveny, R.A.K. Tahirkheli, Paleomagnetic chronology, fluvial processes and tectonic implications of the Siwalik deposits near Chinji Village, Pakistan, Journal of Geology 93 (1985) 27–40.
[65] Y. Najman, E. Garzanti, M. Pringle, M. Bickle, J. Stix, I. Khan, Early-Middle Miocene paleodrainage and tectonics in the Pakistan Himalaya, Geological Society of America Bulletin 115 (2003) 1265–1277.
[66] P.K. Zeitler, Cooling history of the NW Himalaya, Pakistan, Tectonics 4 (1985) 127–151.
[67] D.A. Schneider, M.A. Edwards, W.S.F. Kidd, M.A. Khan, L. Seeber, P.K. Zeitler, Tectonics of Nanga Parbat, western Himalaya: synkinematic plutonism within the doubly vergent shear zones of a crustal-scale pop-up structure, Geology 27 (1999) 999–1002.
[68] M.A. Edwards, W.S.F. Kidd, M.A. Khan, D.A. Schneider, Tectonics of the SW Margin of the Nanga-Parbat Haramosh Massif, in: M.A. Khan, P.J. Treloar, M.P. Searle, M.Q. Jan (Eds.), Tectonics of the Nanga Parbat Syntaxis and the Western Himalaya, vol. 170, Geological Society of London Special Publications, London, 2000, pp. 77–100.
[69] P.O. Koons, P.K. Zeitler, C.P. Chamberlain, D. Craw, A.S. Meltzer, Mechanical links between erosion and metamorphism in Nanga

Parbat, Pakistan Himalaya, American Journal of Science 302 (2002) 749–773.

[70] P.K. Zeitler, P.O. Koons, M.P. Bishop, C.P. Chamberlain, D. Craw, M.A. Edwards, S. Hamidullah, M. Qasim Jan, M. Asif Khan, M.U. Khan Khattak, W.S.F. Kidd, R.L. Mackie, A.S. Meltzer, S.K. Park, A. Pecher, M.A. Poage, G. Sarker, D.A. Schneider, L. Seeber, J.F. Shroder, Crustal reworking at Nanga Parbat, Pakistan: metamorphic consequences of thermal–mechanical coupling facilitated by erosion, Tectonics 20 (2001) 712–728.

[71] D.W. Burbank, J. Leland, E. Fielding, R.S. Anderson, N. Brozovic, M.R. Reid, C. Duncan, Bedrock incision, rock uplift and the threshold hillslopes in the northwestern Himalayas, Nature 379 (1996) 505–510.

[72] D.M. Winslow, P.K. Zeitler, C.P. Chamberlain, L.S. Hollister, Direct evidence for a steep geotherm under conditions of rapid denudation, Western Himalaya, Pakistan, Geology 22 (1994) 1075–1078.

[73] P.K. Zeitler, C.P. Chamberlain, H.A. Smith, Synchronous anatexis, metamorphism, and rapid denudation at Nanga Parbat (Pakistan Himalaya), Geology 21 (1993) 347–350.

[74] M. George, S. Reddy, N. Harris, Isotopic constraints on the cooling history of the Nanga Parbat–Haramosh Massif and Kohistan arc, western Himalaya, Tectonics 14 (1995) 237–252.

[75] D.M. Whipp Jr., T.A. Ehlers, A.E. Blythe, K.W. Huntington, K.V. Hodges, D.W. Burbank, Plio–Quaternary exhumation history of the central Nepalese Himalaya: 2. Thermo-kinematic and thermochronometer age prediction model, Tectonics (in press), doi:10.1029/2006TC001991.